X-ray Absorption Spectroscopy of the Molybdenum Site of *Escherichia coli* Formate Dehydrogenase

Graham N. George,*,† Christopher M. Colangelo,‡ Jun Dong,‡ Robert A. Scott,*,‡ Sergei V. Khangulov,§ Vadim N. Gladyshev,§ and Thressa C. Stadtman*,§

Contribution from the Stanford Synchrotron Radiation Laboratory, SLAC, Stanford University, P.O. Box 4349, MS 69, Stanford, California 94309-0210, the Department of Chemistry and Center for Metalloenzyme Studies, University of Georgia, Athens, Georgia 30602-2556, and the National Institutes of Health, Bethesda, Maryland 20892

Received August 26, 1997

Abstract: X-ray absorption spectroscopy at the molybdenum and selenium K-edges has been used to probe the active site structure of *Escherichia coli* formate dehydrogenase H. The active sites of both oxidized and reduced wild-type protein, and of a variant containing cysteine instead of selenocysteine, were studied. The oxidized and reduced enzymes were found to be very similar, both containing a novel *des*-oxo molybdenum site, with four Mo−S ligands at 2.35 Å, (probably) one Mo−O at 2.1 Å, and one Mo−Se ligand at 2.62 Å being indicated from the Mo K-edge data. The selenium K-edge EXAFS not only is in good agreement with the Mo K-edge data but also indicates the unexpected presence of Se−S ligation, with a bond length of 2.19 Å. We suggest that the active site of *Escherichia coli* formate dehydrogenase H contains a novel seleno-sulfide ligand to molybdenum, where the selenium and sulfur originate from selenocysteine and one of the pterin-cofactor dithiolenes, respectively.

Introduction

The molybdenum enzymes comprise a group with diverse functionality, which catalyze a variety of two-electron redox reactions in which the molybdenum cycles between the Mo^{VI} and Mo^{IV} oxidation states.[1] With the sole exception of nitrogenase, all molybdenum enzymes described to date contain a novel pterin-molybdenum cofactor[2] in which the molybdenum is bound by a dithiolene side chain of the pterin ring (Figure 1). Either one or two pterins are associated with the metal,[3−6] depending upon the enzyme.

Formate dehydrogenases (EC 1.2.1.2) catalyze the oxidation of formate to carbon dioxide:

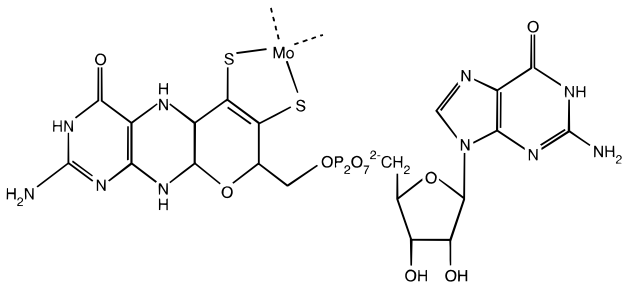

Figure 1. Proposed minimal structure of the molybdenum cofactor. The reversible formation of tricycle via the formation of a pyran ring through attack of the 3′-OH at C-7 of a dihydropterin has been proposed [*e.g.*, see ref 6]. In enzymes from prokaryotic sources the cofactor can have a dinucleotide moeity (cytosine, adenine or guanine dinucleotides are known) attached via the pyrophosphate linkage. The form shown is the guanine dinucleotide.

$$HCOO^- \rightarrow CO_2 + H^+ + 2e^-$$

Formate dehydrogenase H from *Escherichia coli* is the terminal member in the respiratory pathway when the organism is grown anaerobically on glucose. The enzyme is unusual in that it contains a selenocysteine residue (SeCys140) which is essential for full activity and which has been shown by electron paramagnetic resonance (EPR) spectroscopy to be ligated to molybdenum.[7]

Gladyshev *et al.*[7] have compared the amino acid sequence of formate dehydrogenase with a number of other prokaryotic molybdenum enzymes. These workers found that the selenocysteine was contained in a domain of conserved amino acids, being replaced by cysteine in formate dehydrogenases from

* Authors to whom correspondence should be addressed.
† Stanford Synchrotron Radiation Laboratory.
‡ University of Georgia.
§ National Institutes of Health.

(1) (a) Kisker, C.; Shindelin, H.; Rees, D. C. *Annu. Rev. Biochem.* **1997**, *66*, 233−267. (b) Hille, R. *Chem. Rev.* **1996**, 2757−2816. (c) Hille, R. *Biochim. Biophys. Acta* **1994**, *1184*, 143−169. (d) Enemark, J. H.; Young, C. G. *Adv. Inorg. Chem.* **1993**, *40*, 1−88. (e) Bray, R. C. *Quart. Rev. Biophys.* **1988**, *21*, 299−329. (f) Cramer, S. P. *Advances in Inorganic and Bioinorganic Mechanisms*; Sykes, A. G., Ed.; Academic Press; London, 1983; Vol. 2, pp 259−316. (g) Bray, R. C. *Adv. Enzymol. Relat. Areas Mol. Biol.* **1979**, 107−165.

(2) (a) Rajagopalan, K. V. *Adv. Enzymol. Relat. Areas Mol. Biol.* **1991**, *64*, 215−290. (b) Rajagopalan, K. V.; Johnson, J. L. *J. Biol. Chem.* **1992**, 267, 10199−10202.

(3) Hilton, J.; Rajagopalan, K. V. *Arch. Biochem. Biophys.* **1996**, *325*, 139−141.

(4) Schindelin, H.; Kisker, C.; Hilton, J.; Rajagopalan, K. V.; Rees, D. C. *Science* **1996**, *272*, 1615−1621.

(5) (a) Romão, M. J.; Archer, M.; Moura, I.; Moura, J. J. G.; LeGall, J.; Engh, R.; Schneider, M.; Hof, P.; Huber, R. *Science* **1995**, *270*, 1170−1176. (b) Huber, R.; Hof, P.; Duarte, R. O.; Moura, J. J. G.; Moura, I.; Liu, M.-H.; LeGall, J.; Hille, R.; Archer, M.; Romão, M. J. *Proc. Natl. Acad. Sci. U.S.A.* **1996**, *93*, 8846−8851.

(6) Chan, M. K.; Mukund, S.; Kletzin, A.; Adams, M. W. W.; Rees, D. C. *Science* **1995**, *267*, 1463−1469.

(7) Gladyshev, V. N.; Khangulov, S. V.; Axley, M. J.; Stadtman, T. C. *Proc. Natl. Acad. Sci. U.S.A.* **1994**, *91*, 7708−7711.

S0002-7863(97)03004-7 CCC: $15.00
Published on Web 01/30/1998

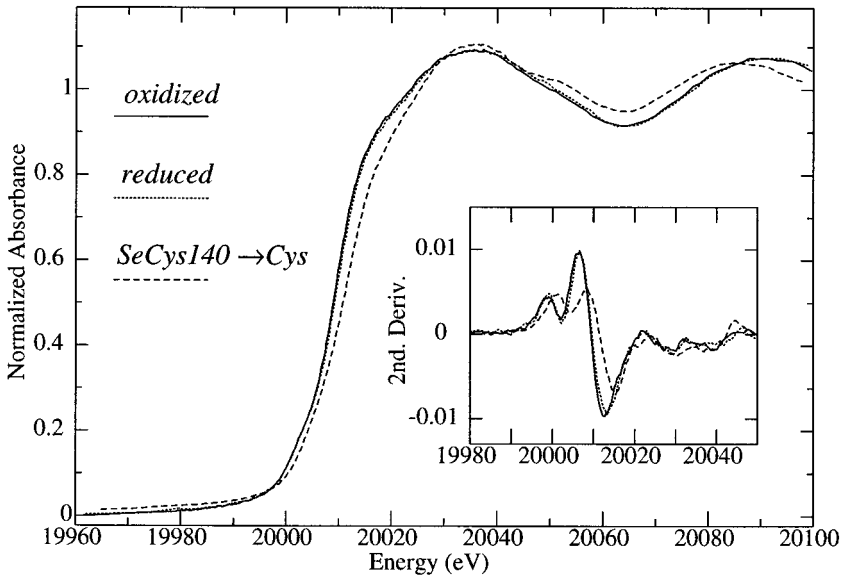

Figure 2. Molybdenum K-edge near-edge spectra of *E. coli* formate dehydrogenase H. Data for the wild-type oxidized and reduced protein, and the SeCys140→Cys mutant are shown. The inset shows the second derivatives of the spectra.

Wolinella succinogenes and *Methanobacterium formicicum* and in nitrate reductases from a variety of sources and being replaced by serine in dimethylsulfoxide reductases and biotin sulfoxide reductase. These workers concluded that these amino acids were likely to be ligands to molybdenum in the other enzymes, and for dimethylsulfoxide reductase recent X-ray crystallography has confirmed that Serine 147 is indeed a molybdenum ligand.[4]

Recently, the X-ray crystal structure of *E. coli* formate dehydrogenase H in both oxidized and formate reduced forms has been reported at 2.9 Å resolution by Boyington *et al.*[8] The structures of both the oxidized and reduced molybdenum sites are reported to be *des*-oxo species, with two cofactor dithiolene ligands and with selenocysteine coordinated to molybdenum. We describe herein an X-ray absorption spectroscopy (XAS) study of the active site of *E. coli* formate dehydrogenase H and of a mutant containing cysteine instead of selenocysteine. This has allowed a structural characterization of the molybdenum site that complements the recent crystallographically determined structure.[8]

Experimental Section

Sample Preparation. Wild type and mutant formate dehydrogenase H samples were purified using a scaled-up version[9] of the procedure of Axley *et al.*[10] *E. coli* strain FM911 containing plasmid pFM20 served as a source of wild-type FDH_H[11] and *E. coli* strain WL31153 containing plasmid pFM201 was the source of the SeCys140→Cys mutant FDH_H.[12] Due to the extreme oxygen sensitivity of (reduced) FDH_H, all procedures were performed under strictly anaerobic conditions (<1 ppm O_2). Enzyme samples were prepared in 60 mM phosphate buffer pH 6.5, with 3 mM sodium azide and 35% v/v glycerol, frozen in lucite sample cuvettes, transported to Stanford on dry ice and stored under liquid nitrogen until data collection. The oxidized and dithionite reduced wild-type FDH_H samples had a final concentration of 2.0 mM and the SeCys140→Cys formate dehydrogenase mutant 2.3 mM. The oxidized sample (initially Mo^V EPR silent) gave characteristic Mo^V EPR signals[7] upon additon of excess formate, strongly suggesting that the oxidized sample was in the fully oxidized Mo^{VI} state. Aliquots of the same (oxidized) preparation retained full activity after being incubated in air for 1 h, which, as the reduced enzyme is unstable in O_2, confirms that the sample was fully oxidized.

Activities of wild-type and mutant FDH_H samples were determined using standard assay conditions[10] as 901 and 5.7 μmol/min per mg protein, respectively. Metal stoichiometries were determined using atomic absorption spectroscopy to be Mo:0.9, Se:1.0, Fe:3.7 for the wild-type and Mo:1.0, Se:<0.05, Fe:4.3 for the mutant.

XAS Data Collection. Selenium and molybdenum K-edge X-ray absorption spectroscopic data were collected at the Stanford Synchrotron Radiation Laboratory (SSRL) with the SPEAR storage ring containing 50−100 mA at 3.0 GeV. The unfocussed wiggler beam line 7-3 was used with a wiggler field of 1.8 T, a Si(220) double crystal monochromator, and an upstream vertical aperture of 1 mm. Harmonic rejection was accomplished by detuning one monochromator crystal to approximately 50% off peak. The incident X-ray intensity was monitored using an argon (for Mo) or nitrogen (for Se) filled ionization chamber, and X-ray absorption was measured as the X-ray K_α fluorescence excitation spectrum with an array of 13 germanium detectors.[13] Samples were maintained at a temperature of approximately 10 K during data collection using an Oxford Instruments liquid helium flow cryostat. Thirteen 20-min scans were accumulated for each sample, and the absorption of a standard metal foil was measured simultaneously by transmittance. The X-ray energy was calibrated with reference to the lowest energy inflection point of the foil spectrum, which was assumed to be 20 003.9 eV for molybdenum metal and 12 656 eV for gray hexagonal selenium.

XAS Data Analysis. The extended X-ray absorption fine structure (EXAFS) oscillations $\chi(k)$ were quantitatively analyzed by curve-fitting with the EXAFSPAK suite of computer programs[14] using *ab initio* theoretical phase and amplitude functions generated with the program *feff* version 7.00.[15] No smoothing, Fourier filtering, or related manipulation was performed upon the data.[16] The values for the

(8) Boyington, J. C.; Gladyshev, V. N.; Khangulov, S. V.; Stadtman, T. C.; Sun, P. D. *Science* **1997**, *275*, 1305−1308.
(9) Gladyshev, V. N.; Boyington, J. C.; Khangulov, S. V.; Grahame, D. A.; Stadtman, T. C.; Sun, P. D. *J. Biol. Chem.* **1996**, *271*, 8095−8100.
(10) Axley, M. J.; Grahame, D. A.; Stadtman, T. C. *J. Biol. Chem.* **1990**, *265*, 18213−18218.
(11) Zinoni, F.; Birkmann, A.; Leinfelder, W.; Böck, A. *Proc. Natl. Acad. Sci. U.S.A.* **1987**, *84*, 3156−3160.
(12) Axley, M. J.; Böck, A.; Stadtman, T. C. *Proc. Natl. Acad. Sci. U.S.A.* **1991**, *88*, 8450−8454.
(13) Cramer, S. P.; Tench, O.; Yocum, M.; George, G. N. *Nucl. Instrum. Methods Phys. Res.* **1988**, *A266*, 586−591.
(14) The EXAFSPAK program suite was developed by one of the authors (G.N.G.) and is available on the SSRL Web site http://ssrl01.slac.stanford.edu/exafspak.html or by application to G.N.G. in writing.
(15) (a) Rehr, J. J.; Mustre de Leon, J.; Zabinsky, S. I.; Albers, R. C. *J. Am. Chem. Soc.* **1991**, *113*, 5135−5140. (b) Mustre de Leon, J.; Rehr, J. J.; Zabinsky, S. I.; Albers, R. C. *Phys. Rev.* **1991**, *B44*, 4146−4156.

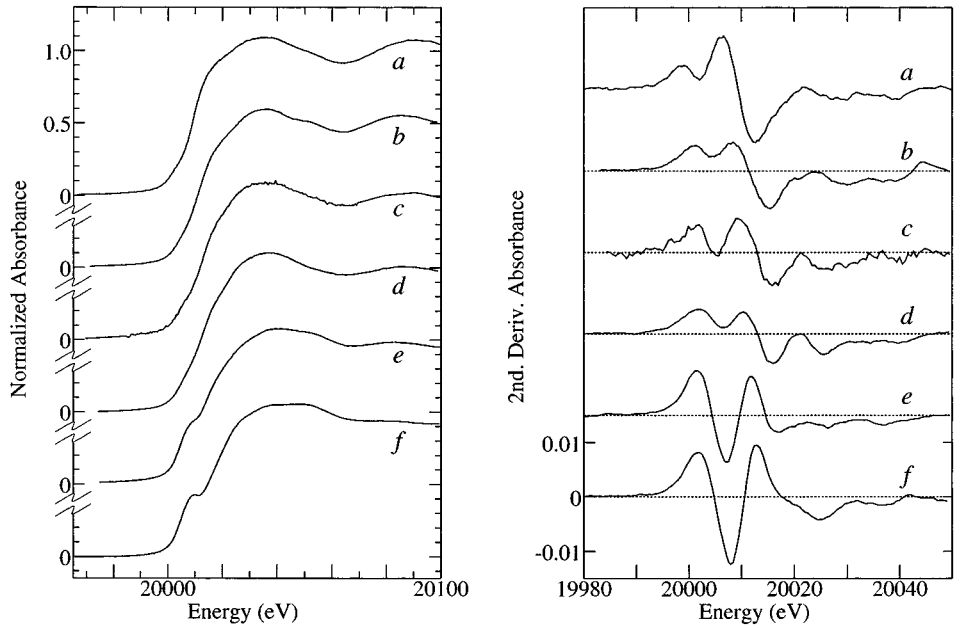

Figure 3. Molybdenum K-edge near-edge spectra (left) and second derivatives (right) of *E. coli* formate dehydrogenase H and related molybdenum enzymes. ***a*** shows the spectrum from wild-type oxidized *E. coli* formate dehydrogenase, ***b*** that of oxidized SeCys140→Cys *E. coli* formate dehydrogenase mutant, ***c*** the spectrum of *E. coli* nitrate reductase,[19] ***d*** that of *Rhodobacter sphaeroides* dimethylsulfoxide reductase,[18] ***e*** that of human sulfite oxidase,[20] and ***f*** that of desulfo xanthine oxidase.[21]

threshold energy (*i.e.*, energy zero for *k*) were assumed to be 20 025 and 12 675 eV for Mo K-edge and Se K-edge data, respectively.

Results and Discussion

Near-Edge Spectra. Figure 2 shows the Mo K-edge near-edge spectra of the oxidized and reduced wild-type *E. coli* formate dehydrogenase, together with the spectrum of the oxidized SeCys140→Cys formate dehydrogenase mutant. The spectra are broadly similar, with only very subtle differences between the oxidized and reduced proteins, but with a somewhat larger difference between the mutant and wild-type data (highlighted by the derivative plot shown in the inset). The spectrum of the mutant is shifted by approximately 2 eV to higher energy, with differences in the intensities and shapes of some features. An increase in edge position might be expected when sulfur is substituted for selenium due to the greater donor capacity of the latter ligand. None of the spectra have the pronounced pre-edge feature at about 20 008 eV that is commonly observed in some other molybdenum enzymes.[17] This so-called oxo-edge feature is characteristic of a species possessing Mo═O groups (or to a lesser extent Mo═S); it arises from formally dipole forbidden 1s → 4d bound-state transitions to antibonding orbitals directed principally along Mo═O bonds.[18] The weak presence of this feature here argues for a low number (*i.e.*, one or zero) of these ligands in the present samples. Figure 3 shows a comparison of the Mo K-edge near-edge spectra of wild-type *E. coli* formate dehydrogenase H, the SeCys140→Cys formate mutant, and those of four related molybdenum enzymes, dimethyl sulfoxide reductase,[18] *E. coli* nitrate reductase,[19] human sulfite oxidase,[20] and desulfo xanthine oxidase.[21] Both dimethyl sulfoxide reductase and nitrate reductase have been shown to possess a mono-oxo Mo^{VI} active site.[18,19] We note some similarity between the spectra of these two enzymes (Figure 3c,d) and that of the mutant (Figure 3b), while the spectrum of the wild-type FDH_H (Figure 3a) appears more distinct (note especially the increased sharpness of the feature centered at about 20 010 eV). As expected, the spectra of sulfite oxidase and desulfo xanthine oxidase (Figure 3e,f), both of which contain dioxo molybdenum active sites, show strong oxo-edge features.

The selenium K-edge near-edge spectra of oxidized and reduced *E. coli* formate dehydrogenase H are compared in Figure 4. Both spectra have an intense feature at 12 659 eV (predominantly transitions from 1s to the partly filled 4p levels), which has a somewhat lower intensity in the reduced sample. The SeCys140→Cys mutant protein showed no selenium K-edge (not illustrated), confirming the lack of any selenium in the variant.

EXAFS Spectra. Figure 5 shows the Mo K-edge EXAFS spectra of oxidized and reduced FDH_H and the SeCys140→Cys mutant, together with the best fits and corresponding EXAFS Fourier transforms. The results of the curve-fitting analyses are summarized in Table 1. For all samples the EXAFS is dominated by intense Mo−S backscattering, giving rise to the Fourier transform peak at about 2.4 Å. For the two wild-type samples (Figure 5B, two top traces) the smaller peak at approximately 2.6 Å is predominantly due to Mo−Se backscattering (some superimposed transform contributions arise due to ringing, or series termination artifacts, from the intense Mo−S backscattering). No short Mo═O interactions were found to

(16) The analysis of the Se K-edge data was complicated by the presence of a very small step in the data at the Pb L_{III} edge (13038eV) presumably arising from lead shielding in the experimental setup or beamline. This was removed from the data by difference, but we note that no difference in the analysis was observed when this was not done, other than physically unreasonable (negative) Debye-Waller factors for the Se−C interactions.

(17) (a) Kutzler, F. W.; Natoli, C. R.; Misemer, D. K.; Doniach, S.; Hodgson, K. O. *J. Chem. Phys.* **1980**, *73*, 3274−3288. (b) Kutzler, F. W.; Scott, R. A.; Berg, J. M.; Hodgson, K. O.; Doniach, S.; Cramer, S. P.; Chang, C. H. *J. Am. Chem. Soc.* **1981**, *103*, 6083−6088.

(18) George, G. N.; Hilton, J.; Rajagopalan, K. V. *J. Am. Chem. Soc.* **1996**, *118*, 1113−1117.

(19) George, G. N.; Turner, N. A.; Bray, R. C.; Morpeth, F. F.; Boxer, D. H.; Cramer, S. P. *Biochem. J.* **1989**, *259*, 693−700.

(20) George, G. N.; Garrett, R. M.; Prince, R. C.; Rajagopalan, K. V. *J. Am. Chem. Soc.* **1996**, *118*, 8588−8592.

(21) (a) Cramer, S. P.; Wahl, R.; Rajagopalan, K. V. *J. Am. Chem. Soc.* **1981**, *103*, 8164−8168. (b) Bordas, J.; Bray, R. C.; Garner, C. D.; Gutteridge, S. P.; Hasnain, S. *Biochem. J.* **1980**, *191*, 499.

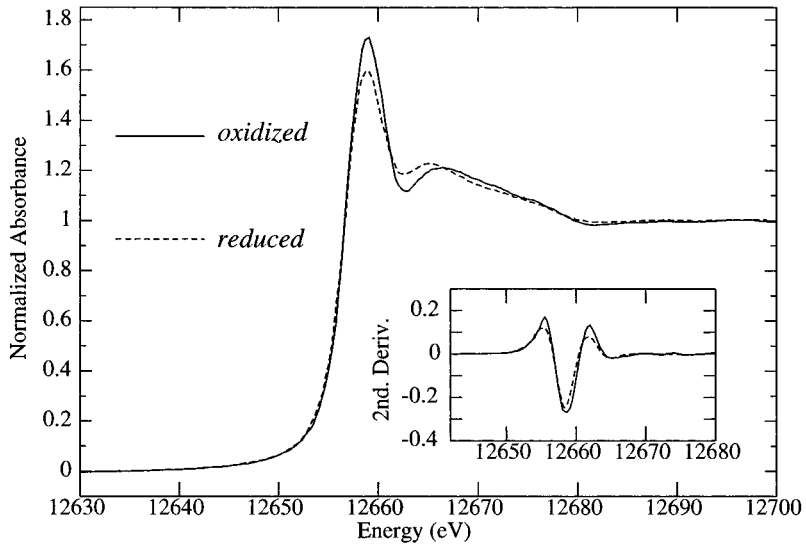

Figure 4. Selenium K-edge near-edge spectra of oxidized and reduced *E. coli* formate dehydrogenase H. The inset shows the second derivatives of the spectra.

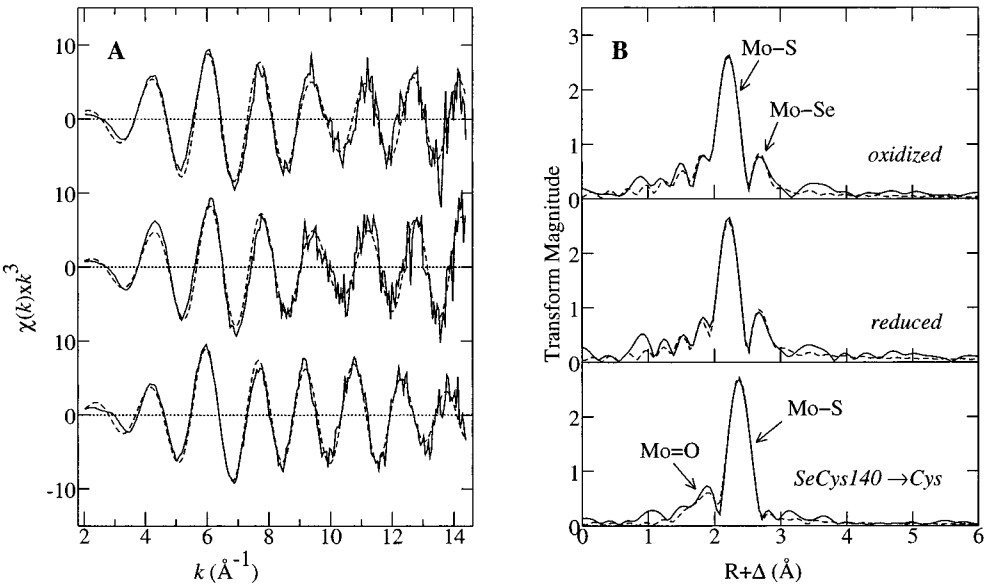

Figure 5. Molybdenum K-edge EXAFS of *E. coli* FDH_H. The solid lines show experimental data, and the broken lines the best fits (Table 1). **A** shows the EXAFS oscillations and **B** shows the corresponding EXAFS Fourier transforms, over the range $k = 2.0-14.2$ Å, phase-corrected for Mo−S backscattering. Features on the low-*R* side of the Mo−S Fourier transform peak of the oxidized and reduced wild-type enzyme are "ringing" effects due to the finite *k*-range of the $\chi(k)$ data and are not due to the presence of any scatterer.

be necessary to fit the oxidized or the reduced wild-type FDH_H EXAFS. In contrast, the SeCys140→Cys mutant does possess a short Mo═O interaction, giving rise to the Fourier transform peak at about 1.8 Å, and, as expected, also lacks the Mo−Se interaction. The Mo−S coordination number is high, being about four for the wild-type FDH_H samples and about five for the SeCys140→Cys mutant (Table 1). This suggests a bis-pterin dithiolene coordination similar to that of dimethyl sulfoxide reductase.[3,4,18] A comparison of the oxidized and dithionite reduced samples indicates very little change in the molybdenum coordination with reduction of the enzyme. This can be illustrated by bond-valence-sum calculations[22,23] (performed as previously described[18]) which yield values of 5.2 for the oxidized sample and 5.8 for the reduced sample, rather than the expected values of 6.0 and 4.0, respectively. In contrast, the oxidized mutant gives a bond-valence-sum of 5.8, which is consistent with a formal Mo^{VI} oxidation state within the expected bond-valence-sum accuracy of ±0.25.[22]

The *des*-oxo Mo^{VI} site is a quite unusual coordination environment for high-valent molybdenum (which might explain the inadequacy of the bond-valence-sum calculations), and its presence in *E. coli* FDH_H extends the previously known structural types for molybdenum active sites (see below).

Figure 6 shows the Se K-edge EXAFS spectra of oxidized and reduced FDH_H, together with the best fits and corresponding EXAFS Fourier transforms. As with the Mo K-edge data the results of the curve-fitting analysis are summarized in Table 1. The Se K-edge EXAFS of both oxidized and reduced samples is dominated by a large Se−Mo backscattering, which gives rise to the Fourier transform peak at about 2.5 Å. From previous EPR spectroscopy,[7] ligation of selenocysteine to molybdenum is expected, and the anticipated ligands to Se are thus carbon and molybdenum. Surprisingly, for both the oxidized and the

(22) (a) Brown, I. D.; Altermat, D. *Acta. Crystallogr.* **1985**, *B41*, 244−247. (b) Brese, N. E.; O'Keeffe, M. *Acta. Crystallogr.* **1991**, *B47*, 192−197.

(23) Thorp, H. H. *Inorg. Chem.* **1992**, *31*, 1583−1588.

Table 1. EXAFS Curve Fitting Results[a]

sample										
Mo−Se			Mo−S			Mo−O[b]				
N	*R*	σ^2	*N*	*R*	σ^2	*N*	*R*	σ^2	E_0	error[c]
					Oxidized Wild-type					
1	2.601(6)	0.0041(5)	3	2.348(4)	0.0010(2)				−17.3(11)	0.379
1	2.616(5)	0.0038(4)	4	2.351(3)	0.0023(1)				−16.8(8)	0.346
1	2.628(5)	0.0037(4)	5	2.354(3)	0.0034(1)				−16.3(7)	0.346
1	**2.621(6)**	**0.0034(4)**	**4**	**2.356(4)**	**0.0021(2)**	**1**	**2.105(19)**	**0.0021(2)**	**−16.3(11)**	**0.333[d]**
1	2.627(6)	0.0034(5)	5	2.355(4)	0.0032(2)	1	2.075(20)	0.0025(2)	−16.8(10)	0.342
			4	2.347(4)	0.0032(3)	1	2.148(27)	0.0033(3)	−18.8(12)	0.429
					Reduced Wild-type					
1	2.603(6)	0.0037(5)	3	2.343(3)	0.0012(2)				−15.0(10)	0.381
1	2.613(5)	0.0036(4)	4	2.344(3)	0.0024(1)				−15.1(8)	0.351
1	2.625(4)	0.0033(3)	5	2.348(3)	0.0036(1)				−14.4(7)	0.346
1	**2.618(6)**	**0.0033(4)**	**4**	**2.349(4)**	**0.0024(2)**	**1**	**2.093(32)**	**0.0057(28)**	**−14.4(11)**	**0.344[d]**
1	2.619(5)	0.0032(4)	5	2.343(3)	0.0035(2)	1	2.024(22)	0.0059(29)	−15.4(8)	0.351
			4	2.326(5)	0.0029(2)	1	2.004(28)	0.0060(32)	−19.5(14)	0.449
					Oxidized Mutant					
			3	2.412(2)	0.0013(1)	1	1.711(5)	0.0021(5)	−12.3(7)	0.290
			4	2.415(2)	0.0026(1)	1	1.716(4)	0.0024(4)	−11.5(5)	0.232
			5	**2.417(2)**	**0.0036(1)**	**1**	**1.719(4)**	**0.0026(4)**	**−10.9(4)**	**0.224[d]**
			6	2.419(2)	0.0047(1)	1	1.723(5)	0.0027(5)	−10.3(5)	0.253
			5	2.416(2)	0.0037(1)	2	1.718(4)	0.0067(5)	−10.9(5)	0.243
Se−Mo			Se−C			Se−S				
N	*R*	σ^2	*N*	*R*	σ^2	*N*	*R*	σ^2	E_0	error[c]
					Oxidized Wild-type					
1	2.604(8)	0.0033(3)	1	2.050(10)	−0.0006(7)				−16.4(25)	0.547
1	**2.617(7)**	**0.0030(2)**	**1**	**1.959(9)**	**0.0021(2)**	**1**	**2.193(3)**	**0.0023(3)**	**−13.8(23)**	**0.386[d]**
					Reduced Wild-type					
1	2.608(3)	0.0043(2)	1	2.058(6)	0.0004(6)				−14.4(23)	0.524
1	**2.615(2)**	**0.0045(2)**	**1**	**1.983(14)**	**0.0052(19)**	**1**	**2.199(5)**	**0.0047(6)**	**−10.4(6)**	**0.397[d]**

[a] Coordination number *N*, interatomic distance *R* (Å), and (thermal and static) mean-square deviation in *R* (the Debye-Waller factor) σ^2 (Å^2). The values in parentheses are the estimated standard deviations (precisions) obtained from the diagonal elements of the covariance matrix. We note that the accuracies will always be somewhat larger than the precisions, typically ±0.02 Å for *R* and ±20% for *N* and σ^2. [b] Note that EXAFS cannot readily distinguish between scatterers of similar atomic number, such as chlorine and sulfur or nitrogen and oxygen. [c] The fit-error is defined as $\sum k^6(\chi_{exptl} - \chi_{calcd})^2/\sum k^6\chi_{exptl}^2$. [d] Fits shown in bold type-face represent the best fit obtained for the sample.

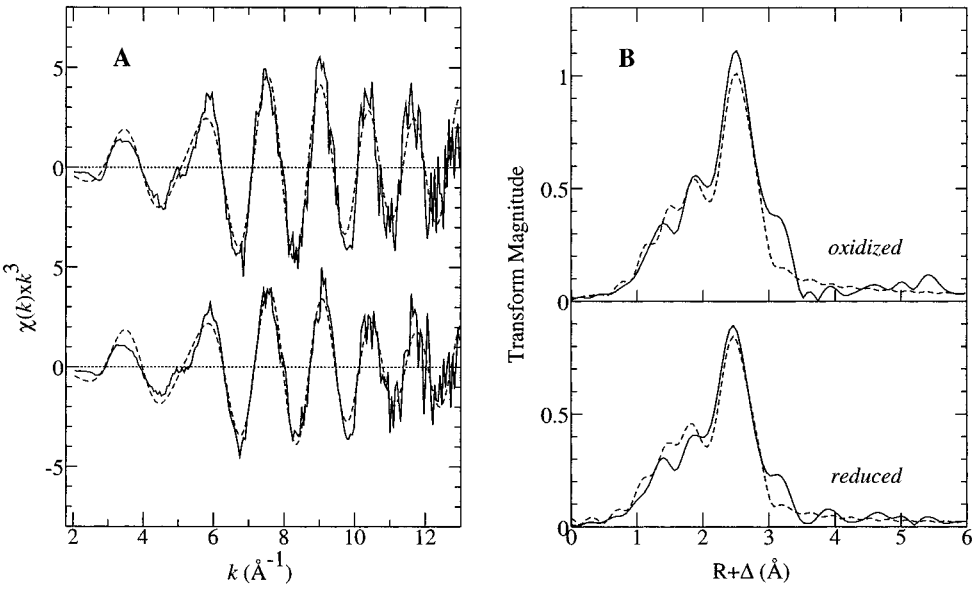

Figure 6. Selenium K-edge EXAFS of *E. coli* FDH_H. The solid lines show experimental data, and the broken lines show the best fits (Table 1). **A** shows the EXAFS oscillations and **B** shows the corresponding EXAFS Fourier transforms, over the range $b = 2.0-13.0$ Å, phase-corrected for Se−Mo backscattering.

reduced samples, we find that it is not possible to adequately fit the data with Se−C and Se−Mo alone. An additional ligand to selenium, most likely sulfur, is required. Figure 7 compares the Se K-edge EXAFS Fourier transforms and best-fits for oxidized FDH_H with and without the inclusion of the Se−S interaction. The top inset to the figure shows a search profile, calculated by performing a series of fits for various Se−S coordination numbers, and a very pronounced minimum can

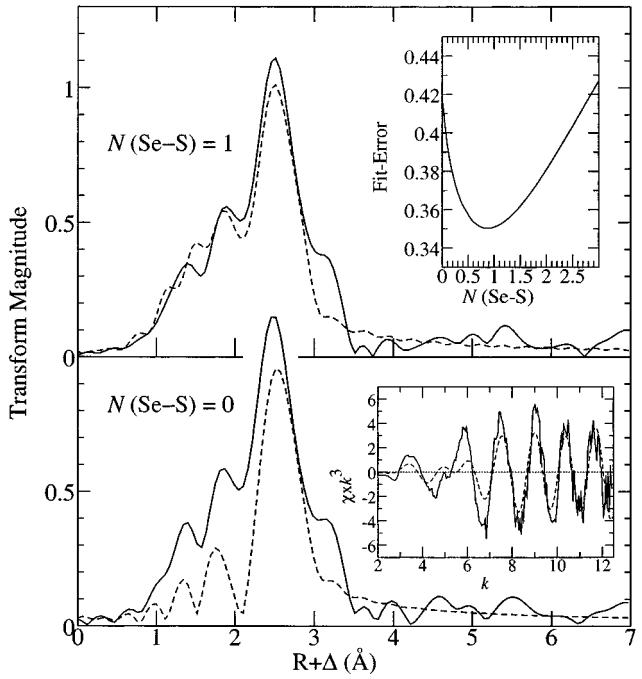

Figure 7. Se K-edge EXAFS Fourier transforms of the oxidized *E. coli* FDH_H illustrating the goodness of fit attainable with and without Se−S coordination. The transforms were calculated using Se−Mo phase-correction. The top inset shows a search profile for Se−S coordination number, calculated by refining all parameters except for Se−S coordination number, which was varied systematically over the range shown on the abscissa of the plot. The bottom inset shows the best fit to the Se EXAFS data without inclusion of Se−S. In all parts of the figure the solid lines show experimental data, and the broken lines are the calculated curves.

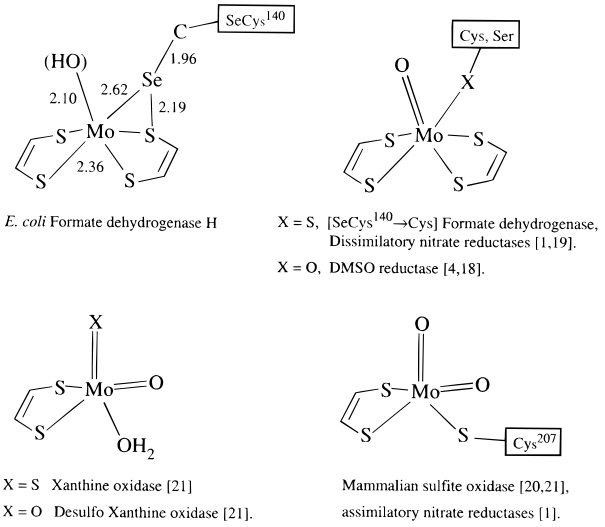

Figure 8. Proposed structures for the molybdenum active sites of oxidized wild-type FDH_H and the oxidized SeCys140→Cys mutant, compared to active sites of related molybdenum enzymes. We note that geometric information is not directly available from the present EXAFS analysis.

be seen for a Se−S coordination number of about 0.9 (*i.e.*, one within the limits of the EXAFS uncertainty).

Figure 8 shows proposed active site structures for the wild-type enzyme and for the SeCys140→Cys mutant. In the figure we postulate a triangular arrangement of Mo, S, and Se. Such sideways-on coordination, while not previously suggested in molybdenum enzymes, is quite well-known in $Mo(S_2)$, $Mo(Se_2)$ and Mo(RSSR) complexes, in addition to Mo(SeS) compounds.[24] The EXAFS derived Se−S distance of 2.19 Å is well within the range of 2.15−2.23 Å expected for this type of ligand to molybdenum.[24] We note that a molybdenum dithiolene model complex with a disulfide linkage (S−S of 2.08 Å) has been described[25] although, with different coordination to Mo than that suggested in Figure 8. An alternative possible source of the sulfur coordination to selenium is a protein cysteine residue. *E. coli* FDH_H contains an unusual dicysteinyl (Cys135−Cys136) arrangement near to the conserved selenocysteine residue.[7,26] This sequence, however, is not conserved,[27] and as the crystallographically-determined fold of the polypeptide chain suggests an unfavorable location for selenium coordination,[8] we consider this possibility unlikely. A further possibility is that the enzyme contains an additional sulfur, perhaps related to the cyanolysable terminal sulfide[28] of the molybdenum hydroxylases,[1] which is coordinated to both Mo and Se. Again, we consider this alternative unlikely, as the crystal structure would probably have detected such an additional sulfur atom.

We note that the presence of Se−S coordination means that the active site may be capable of accepting a total of four electrons, two to reduce Mo^{VI} to Mo^{IV} and two to reduce the selenosulfide bond.

While this work was in progress, the crystal structure of *E. coli* FDH_H was reported to 2.9 Å resolution by Boyington *et al.*[8] This work confirmed the previous conclusions from EPR spectroscopy that selenocysteine is a ligand of molybdenum[7] and also showed that the other ligands to Mo were two pterin dithiolenes (a total of four Mo−S ligands) and a single Mo−OH in the oxidized enzyme. The crystallographic analysis indicated Mo−S distances of 2.6, 2.3, 2.4, and 2.4 Å for the oxidized enzyme and 2.1, 2.3, 2.5, and 2.3 Å for the formate reduced enzyme.[8] The active site structure of the formate reduced enzyme (studied crystallographically) is likely to be somewhat different from that of the dithionite reduced protein studied in the present work; however, the oxidized samples should be directly comparable. As described thus far, and allowing for the crystallographic accuracy of about a few tenths of an Ångström, and the EXAFS accuracy of about 0.02 Å, these conclusions are in reasonable agreement with the present work. In marked contrast, however, is the fact that the crystallographic analysis did not detect any Se−S ligation. For the oxidized enzyme the closest crystallographic Se−S separation was determined as 2.8 Å, and for the formate reduced enzyme, as 3.1 Å. While both distances are shorter than the sum of van der Walls radii, suggesting a partial Se···S bond, these interatomic distances are in marked contrast with the EXAFS-determined Se−S bond length of 2.19 Å.

As discussed by Rees and co-workers,[29] determination of exact interatomic distances from protein crystallography can often be difficult, especially when a heavy scatterer such as a

(24) (a) Fedin, V. P.; Sokolov, M. N.; Virovets, A. V.; Podberezskaya, N. V.; Federov, V. E. *Polyhedron* **1992**, *11*, 2395−2398. (b) Fedin, V. P.; Sokolov, M. N.; Federov, V. E.; Yufit, D. S.; Struchkov, Yu. T. *Inorg. Chim. Acta* **1991**, *179*, 35−40. (c) Fedin, V. P.; Mironov, Yu. V.; Sokolov, M. N.; Kolesov, B. A.; Federov, V. E.; Yufit, D. S.; Struchkov, Yu. T. *Inorg. Chim. Acta* **1990**, *174*, 275−282. (d) Gea, Y. Ph.D. Dissertation, State University of New York at Stony Brook, 1993.

(25) Pilato, R. S.; Eriksen, K. A.; Greaney, M. A.; Stiefel, E. I.; Goswami, S.; Kilpatrick, L.; Spiro, T. G.; Taylor, E. C.; Rheingold A. L. *J. Am. Chem. Soc.* **1991**, *113*, 9372−9375.

(26) Zinoni, F.; Birkmann, A.; Stadtman, T. C.; Böck, A. *Proc. Natl. Acad. Sci. U.S.A.* **1986**, *83*, 4650−4654.

(27) Berg, B. L.; Li, J.; Heider, J.; Steward, V. *J. Biol. Chem.* **1991**, *266*, 22380−22385.

(28) Both wild-type and SeCys140→Cys mutant formate dehydrogenases are irreversibly inactivated by CN^- (Gladyshev, V. N.; Stadtman T. C, unpublished data).

(29) Schindelin, H.; Kisker, C.; Rees, D. C. *JBIC* **1997**, in press.

Chart 1

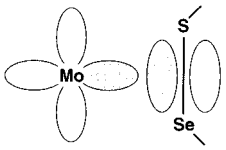

metal or selenium is present. Even allowing for such difficulties, the discrepancy between the crystallography and the EXAFS of at least 0.6 Å for the Se−S interatomic distance is difficult to account for, and it is possible that a difference exists between the *E. coli* FDH_H active site structures in crystalline and frozen solution forms. For example, as suggested above, the Se−S bond should be readily reducible and perhaps this was the form crystallized.[30] In any case, the EXAFS data presented here clearly demonstrate the presence of Se−S ligation in both the oxidized and the dithionite reduced frozen solution samples which were studied.

The formate reduced enzyme gives rise to highly distinctive Mo^V EPR spectra[7] which integrate to between 40 and 60% Mo^V (the remainder presumably being Mo^{IV}). As stated above, formate reduced FDH_H was not studied in this work; however, we will consider the implications of a selenosulfide active site with regard to the Mo^V EPR properties. Examination of the *E. coli* FDH_H Mo^V EPR spectra presented by Gladyshev *et. al.*[7] indicates an unusually large anisotropic ^{77}Se hyperfine coupling. This is much larger than ^{77}Se hyperfine coupling that is observed in Mo^V model compound systems[31] and indicates significant delocalization of the paramagnetic Mo^V 4d electron onto selenium.[32] This is not consistent with a long, isolated, Mo−Se bond, observed crystallographically. It is, however, consistent with Mo−(Se−S) ligation for which overlap between the paramagnetic Mo 4d orbital and Se−S π orbitals (Chart 1) is possible. In this case, the observed large spin delocalization onto selenium (and the seleno-sulfide sulfur) would be expected.[34] Boyington *et al.*[8] have suggested a catalytic mechanism for formate dehydrogenase in which selenocysteine acts as an acceptor for the α proton of formate, and selenosulfide might function in this role, although somewhat less effectively. Alternatively, a role for selenosulfide as a hydride or hydrogen atom acceptor might be suggested by the reducible nature of the seleno-sulfide ligand.

The presence of a seleno-sulfide ligand to Mo in *E. coli* FDH_H suggests the interesting possibility of similar metal ligation in other molybdenum enzymes with sulfur in place of selenium, especially as recent density functional calculations of possible molybdenum enzyme active sites predict that molybdenum disulfide ligation of the form

should be quite stable.[35] In particular, some dissimilatory nitrate reductases possess a cysteine residue in place of the selenocysteine of *E. coli* FDH_H,[1,7] and the possibility should be considered that these enzymes contain a cofactor−S−S−Cys disulfide ligand to molybdenum. The molybdenum of mammalian sulfite oxidase possesses a cysteine ligand,[20,36] which also might form a similar disulfide under some circumstances. We note that partial disulfide bonds, with an S···S distance close to 2.8 Å, have been observed crystallographically both in model compounds[37,38] and in the oxidized molybdenum site of *Desulfovibrio gigas* aldehyde oxidoreductase.[5] Finally, in xanthine oxidase, while the presence of a terminal sulfido (Mo═S) ligand in the oxidized enzyme is well established, it is plausible that the much-studied very rapid intermediate[1,39] might in fact be a disulfide species, rather than, as is commonly supposed, a Mo═S species.

Acknowledgment. The Stanford Synchrotron Radiation Laboratory is funded by the Department of Energy, Office of Basic Energy Sciences. The Biotechnology Program is supported by the National Institutes of Health, Biomedical Research Technology Program, Division of Research Resources. Further support is provided by the Department of Energy, Office of Biological and Environmental Research. We are indebted to Martin J. George of SSRL for use of his data collection software and to Richard Glass and John Enemark, both of the University of Arizona, for helpful comments. XAS research in the RAS laboratory is supported by the NIH (GM42025). C.M.C. received a traineeship from the Center for Metalloenzyme Studies NSF Research Training Group (DIR 90-14281). G.N.G. performed XAS data analysis and most of the writing; C.M.C., J.D., and R.A.S. collected and reduced the XAS data; S.V.K. and V.N.G. provided samples for X.A.S.; T.C.S., R.A.S., G.N.G., and V.N.G. provided intellectual input.

JA973004L

(30) This possibility seems unlikely as the crystals showed a full compliment of enzyme activity after being redissolved in buffer.[8,9]

(31) Hanson, G. R.; Wilson, G. L.; Bailey, T. D.; Pilbrow, J. R.; Wedd, A. G. *J. Am. Chem. Soc.* **1987**, *109*, 2609−2616.

(32) Simulations indicate (^{77}Se)*A* principal values of 234, 56, and 21 MHz, with the smallest coupling being approximately in the direction of the largest *g*-value (slight noncolinearity of **g** and **A** improved the simulations slightly). From the EXAFS and crystallographically derived Mo−Se bond-lengths (2.6 and 2.5 Å, respectively) we expect a dipole contribution to the anisotropic coupling of less than 2 MHz, and using standard arguments,[33] we can calculate an approximate electron density for the paramagnetic Mo 4d electron on selenium of at least 0.2 electrons.

(33) Goodman, B. A.; Raynor, J. B. *Adv. Inorg. Chem. Radiochem.* **1970**, *13*, 135−362.

(34) The largest axis of the resulting anisotropic hyperfine coupling would be directed perpendicular to the Se−S bond, approximately toward the molybdenum.

(35) Bray, M. R.; Deeth, R. J. *Inorg. Chem.* **1996**, *35*, 5720−5724.

(36) Garrett, R. M.; Rajagopalan, K. V. *J. Biol.. Chem.* **1996**, *271*, 7387−7391.

(37) Steifel, E. I.; Miller, K. F.; Bruce, A. E.; Corbin, J. L.; Berg, J. M.; Hodgson, K. O. *J. Am. Chem. Soc.* **1980**, *102*, 3624−3626.

(38) Young, C. G. *JBIC* **1997**, in press.

(39) (a) Howes, B. D.; Bray, R. C.; Richards, R. L.; Turner, N. A.; Bennett, B.; Lowe, D. J. *Biochemistry* **1996**, *35*, 1432−1443. (b) George, G. N.; Bray, R. C. *Biochemistry* **1988**, *27*, 3603−3609.